



1-20-2018

Kinetic Modelling and Experimental Studies for the Effects of Fe²⁺ Ions on Xylan Hydrolysis with Dilute-Acid Pretreatment and Subsequent Enzymatic Hydrolysis

Hui Wei

Xiaowen Chen

Joseph Shekiro

Erik Kuhn

Wei Wang

See next page for additional authors

Follow this and additional works at: <https://commons.und.edu/che-fac>

 Part of the [Chemical Engineering Commons](https://commons.und.edu/che-fac)

Recommended Citation

Wei, Hui; Chen, Xiaowen; Shekiro, Joseph; Kuhn, Erik; Wang, Wei; Ji, Yun; Kozliak, Evguenii; Himmel, Michael E.; and Tucker, Melvin P., "Kinetic Modelling and Experimental Studies for the Effects of Fe²⁺ Ions on Xylan Hydrolysis with Dilute-Acid Pretreatment and Subsequent Enzymatic Hydrolysis" (2018). *Chemical Engineering Faculty Publications*. 7.
<https://commons.und.edu/che-fac/7>


This Article is brought to you for free and open access by the Department of Chemical Engineering at UND Scholarly Commons. It has been accepted for inclusion in Chemical Engineering Faculty Publications by an authorized administrator of UND Scholarly Commons. For more information, please contact zeinebyousif@library.und.edu.

Authors

Hui Wei, Xiaowen Chen, Joseph Shekiro, Erik Kuhn, Wei Wang, Yun Ji, Evguenii Kozliak, Michael E. Himmel, and Melvin P. Tucker

Article

Kinetic Modelling and Experimental Studies for the Effects of Fe²⁺ Ions on Xylan Hydrolysis with Dilute-Acid Pretreatment and Subsequent Enzymatic Hydrolysis

Hui Wei ¹, Xiaowen Chen ^{2,*} , Joseph Shekero ², Erik Kuhn ², Wei Wang ², Yun Ji ³, Evguenii Kozliak ⁴, Michael E. Himmel ¹ and Melvin P. Tucker ²

¹ Biosciences Center, National Renewable Energy Laboratory, 15013 Denver West Parkway, Golden, CO 80401, USA; Hui.Wei@nrel.gov (H.W.); Mike.Himmel@nrel.gov (M.E.H.)

² National Bioenergy Center, National Renewable Energy Laboratory, 15013 Denver West Parkway, Golden, CO 80401, USA; Joseph.Shekero@nrel.gov (J.S.); Erik.Kuhn@nrel.gov (E.K.); Wei.Wang@nrel.gov (W.W.); Melvin.tucker@nrel.gov (M.P.T.)

³ Chemical Engineering Department, University of North Dakota, 241 Centennial Drive, Grand Forks, ND 58202, USA; yun.ji@engr.und.edu

⁴ Chemistry Department, University of North Dakota, 241 Centennial Drive, Grand Forks, ND 58202, USA; evguenii.Kozliak@und.edu

* Correspondence: Xiaowen.Chen@nrel.gov; Tel.: +1-303-384-6828

Received: 1 December 2017; Accepted: 16 January 2018; Published: 20 January 2018

Abstract: High-temperature (150–170 °C) pretreatment of lignocellulosic biomass with mineral acids is well established for xylan breakdown. Fe²⁺ is known to be a cocatalyst of this process although kinetics of its action remains unknown. The present work addresses the effect of ferrous ion concentration on sugar yield and degradation product formation from corn stover for the entire two-step treatment, including the subsequent enzymatic cellulose hydrolysis. The feedstock was impregnated with 0.5% acid and 0.75 mM iron cocatalyst, which was found to be optimal in preliminary experiments. The detailed kinetic data of acid pretreatment, with and without iron, was satisfactorily modelled with a four-step linear sequence of first-order irreversible reactions accounting for the formation of xylooligomers, xylose and furfural as intermediates to provide the values of Arrhenius activation energy. Based on this kinetic modelling, Fe²⁺ turned out to accelerate all four reactions, with a significant alteration of the last two steps, that is, xylose degradation. Consistent with this model, the greatest xylan conversion occurred at the highest severity tested under 170 °C/30 min with 0.75 mM Fe²⁺, with a total of 8% xylan remaining in the pretreated solids, whereas the operational conditions leading to the highest xylose monomer yield, 63%, were milder, 150 °C with 0.75 mM Fe²⁺ for 20 min. Furthermore, the subsequent enzymatic hydrolysis with the prior addition of 0.75 mM of iron(II) increased the glucose production to 56.3% from 46.3% in the control (iron-free acid). The detailed analysis indicated that conducting the process at lower temperatures yet long residence times benefits the yield of sugars. The above kinetic modelling results of Fe²⁺ accelerating all four reactions are in line with our previous mechanistic research showing that the pretreatment likely targets multiple chemistries in plant cell wall polymer networks, including those represented by the C–O–C and C–H bonds in cellulose, resulting in enhanced sugar solubilization and digestibility.

Keywords: pretreatment; enzymatic hydrolysis; bio-ethanol; Lewis acid; iron cocatalyst; kinetics

1. Introduction

Lignocellulosic biomass consists of three major components: cellulose, hemi-cellulose and lignin [1]. It also includes non-cellulosic polysaccharides (such as pectin). The utilization of cellulose and hemi-cellulose for production of ethanol has been studied extensively [2–6]. However, hydrolysis of lignocellulosic biomass into fermentable monosaccharides remains a challenging task due to the notorious biomass recalcitrance [7]. Pretreatment of lignocellulosic biomass with dilute mineral acids under mild conditions has been found to effectively separate and break down hemicellulose, modify the lignin network and increase cellulose accessibility [8,9]. Overall, the technology of dilute-acid pretreatment is being actively studied and applied; in 2017 alone, a number of papers have been published in the field of dilute-acid pretreatment of biomass [10–18].

However, dilute-acid pretreatment faces several challenges, including acid recovery, neutralization of pretreated biomass and the need for acid-resistant reactors whose manufacture requires specific and expensive metallurgy [19,20]. In addition, precise process control is required to avoid the potential rapid degradation of desired monomeric sugars into potent inhibitors of fermentation. Many of these challenges can be mitigated through reduction in both acid loading and reaction temperature. Efficient dilute-acid pretreatment of biomass at mild temperatures (100–130 °C) has been reported recently, which also achieved high conversion of xylan to xylose. These reports included a 2% (*w/v*) sulfuric acid pretreatment of palm frond at 120 °C for 120 min [21], 2.5% sulfuric acid pretreatment of corn stover at 120 °C for 1.5 h [22], and 1.0–1.5% sulfuric or phosphoric acid pretreatment of wheat bran and whole-stillage fibers at 100 °C (using hot water from the first-generation ethanol plants) for 1.0–4.5 h [11].

For this refined pretreatment, iron cocatalysts have been shown to further speed up the xylan hydrolysis and improve xylose yields compared to dilute acid only under the same conditions. Nguyen and Tucker demonstrated a 20–30% improvement in the overall sugar yield from softwood through the incorporation of 0.5–2.0 mM ferrous sulfate during the dilute acid impregnation stage [23]. Liu et al. reported that a pretreatment with 0.1 M ferric chloride alone, with no acids, at 140 °C can remove almost 100% of hemicellulose and recover 89% of xylan as sugar in corn stover [24]. However, Liu and Wyman also found that ferric ions increased the rate of xylose degradation up to 6.1 times and that of xylotriose as much as 49-fold [25]. Chen et al. also reported a pretreatment with FeCl₃ of rice straw with an 83% hemicellulose removal and 82% glucose yield after the subsequent enzymatic hydrolysis [26]. These findings warrant further studies on sugar product yields with iron, and the current study addresses this issue.

Furthermore, evidence was presented that iron salts can also improve cellulose digestibility during enzymatic hydrolysis following the acid pretreatment [27]. When FeCl₃ was incorporated into a sulfuric acid-containing mixture used to neutralize the hydrolysate from an organosolv pretreatment, the enzymatic digestibility was improved by 60% over a control neutralized with H₂SO₄ only [28]. Liu and Zhu postulated that the observed increase is due to the formation of lignin–metal complexes, which may help reduce the affinity of lignin to cellulase enzymes, resulting in improved cellulose accessibility and digestion efficiency [29]. Degenstein et al. studied oligomer saccharide reduction during a dilute-acid pretreatment cocatalyzed with Lewis acids [30]. However, no reports have been published covering the combined effects of iron on both xylose and glucose release and process kinetics.

To assess the rates and mechanism of the acid hydrolysis of xylan, a number of studies have been performed using two kinetic models. The simplest model is a linear two-step consecutive homogeneous pseudo-first-order irreversible reaction (Equation (1)) derived from the study of acid hydrolysis of cellulose [31]. This model was then modified to include oligomer intermediates and the main xylose degradation product, furfural, whose occurrence was confirmed by experimental observations (Equation (2)) [32]. Furthermore, this model was adjusted to a biphasic model of the first step, which assumed the hydrolysis of two fractions of xylan at different reaction rates [33]. However, kinetic modeling of acid/iron pretreatments has not been performed. In this study, a more general four-step

linear irreversible reaction model, Equation (2), was adopted to describe the obtained experimental data and allows for a more detailed mechanistic analysis of xylose formation/breakdown balance.



where

- XH = xylan in biomass;
- XO = xylooligomer;
- X = xylose;
- F = furfural;
- D = degradation products.

The goal of the present work was to determine the effect of ferrous ion concentration on sugar yield and degradation product formation for the entire two-step treatment. Firstly, the detailed kinetic data of acid pretreatment, with and without iron, was fitted into a four-step linear sequence of first-order irreversible reactions shown in Equation (2). Focusing on the mechanistic aspects of the process, the values of Arrhenius activation energy (E_a) were calculated and compared with those found in control experiments and literature. Then, enzymatic hydrolysis of such a pretreated biomass was performed to evaluate the impact of the acid and iron combination on glucose production, thus assessing the total feedstock reactivity.

2. Results

2.1. Effect of Ferrous Ion on Xylan Hydrolysis during Acid Pretreatment

Effects of ferrous ion on acid pretreatment were examined using corn stover, which contained glucan, xylan and lignin in 34%, 22% and 12%, respectively. Other significant components included 4% sucrose, 3% uronic acid, 3% acetate and 8% total extractives. After the dilute acid and cocatalyst impregnation, most of the sucrose was dissolved in the RAPI (recirculating atmospheric pressure impregnation) post-soak liquor, along with some water-soluble extractives. As a result, the proportional glucan, xylan and lignin contents of the impregnated solids increased to 38%, 25% and 18%, respectively (Table 1). The incremental increases are believed to vary due to the differences in solubilities of these components in acid solutions. The conducted mass balance closure indicated that 1% of the original glucan and 2% of the original xylan were lost during impregnation. The addition of an iron cocatalyst did not have a significant effect on the composition of soaked solids when compared to the dilute-acid-impregnated control. The amount of xylan present in the impregnated biomass was recorded in this compositional data and then used for yield calculations.

Table 1. Solids compositional analysis of acid-only and acid cocatalyst-soaked corn stover.

Sample ID	Ash (%)	Lignin (%)	Glucan (%)	Xylan (%)	Galactan (%)	Arabinan (%)	Acetate (%)	Total (%)
0.5% H ₂ SO ₄ only	5.5	18.2	38.4	25.0	1.9	4.3	3.1	96.3
0.5% H ₂ SO ₄ , 0.75 mM FeSO ₄	3.2	18.5	38.3	26.6	1.9	4.0	3.3	95.8
0.5% H ₂ SO ₄ , 1 mM FeSO ₄	5.2	18.4	38.9	24.8	2.6	5.8	3.7	99.3

The xylan mass balance, depicted in Figure 1, successfully closed at 100% ± 5% in all but three instances (control, 5 min; 0.75 mM FeSO₄, 5 min; and control, 10 min), although even in these cases the larger deviations from 100% appeared to have a statistical origin. The observed mass balance discrepancies are thus likely due to experimental and/or analytical errors. The conducted analyses showed that the maximum xylan solubilization was achieved when the feedstock was

impregnated with 0.5% acid and 0.75 mM iron cocatalyst, at the residence times tested. Corroborating this observation, xylooligomer yields were found to be significantly depressed with 1 mM Fe^{2+} . A similar trend was observed for monomeric xylose yields. The observed reduction in pretreatment effectiveness between 0.75 mM and 1 mM Fe^{2+} may be caused by the competition between the Brønsted (H^+) and Lewis (Fe^{2+}) acids. Apparently, they both are essential for achieving a high treatment efficiency.

More than 82% of xylan was solubilized at 150 °C with 0.75 mM Fe^{2+} at both 10 min and 20 min residence times. The highest xylose monomer yield, 63.4%, was achieved at 150 °C with 0.75 mM Fe^{2+} for 20 min. This set of conditions also minimized the amount of xylan remaining in the pretreated solids (15.5%). Meanwhile, approximately 1.9% of xylan was converted to furfural in all experiments (Figure 1).

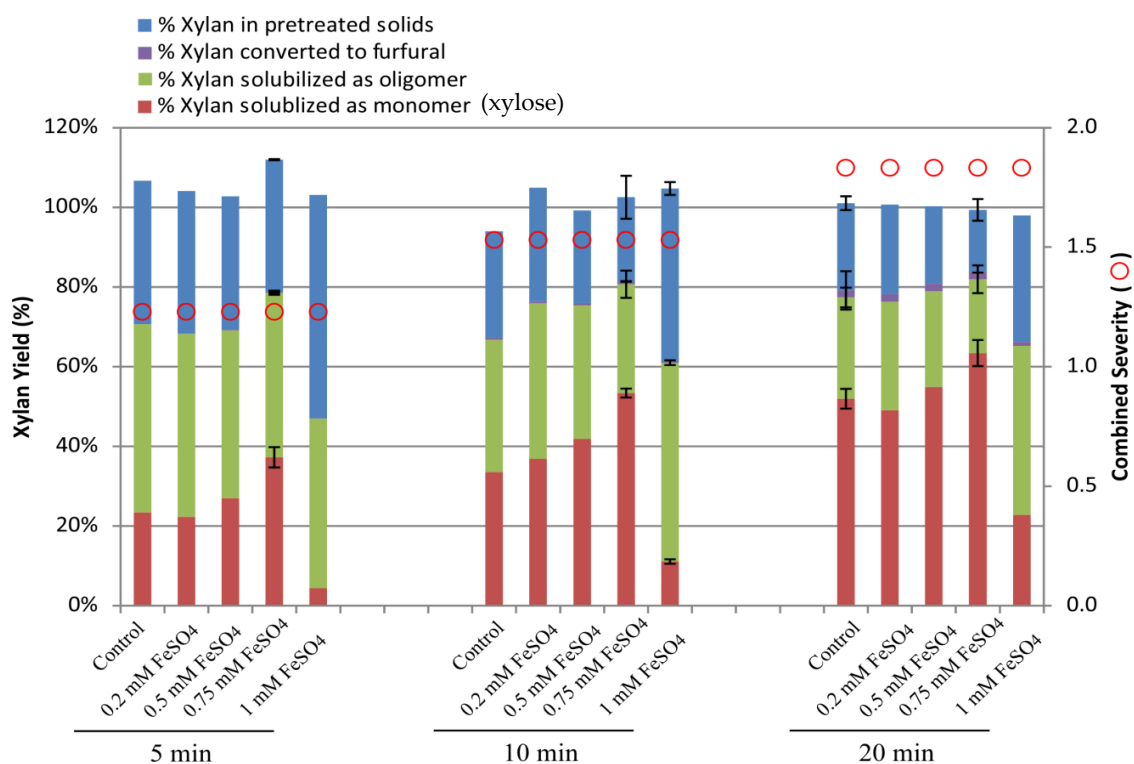


Figure 1. Xylan/xylose mass balance closure for pretreatments at 150 °C and 0.5% H_2SO_4 with increasing levels of FeSO_4 addition.

Figure 2 shows slight yet statistically significant changes in the remaining xylose distribution among various particle sizes that occurred as a result of the presence of iron in the pretreatment medium. The greater fraction of xylose in smaller particles observed in the presence of iron cannot be solely attributed to an increase in the treatment efficiency, as the increase of duration of the iron-free treatment did not result in similar changes. It could indicate a higher overall pretreatment severity caused by iron.

This initial study indicated that the biomass impregnation with 0.5% acid and 0.75 mM ferrous sulfate was optimal, and these conditions were used for further experimentation at 160 °C and 170 °C to obtain kinetic parameters.

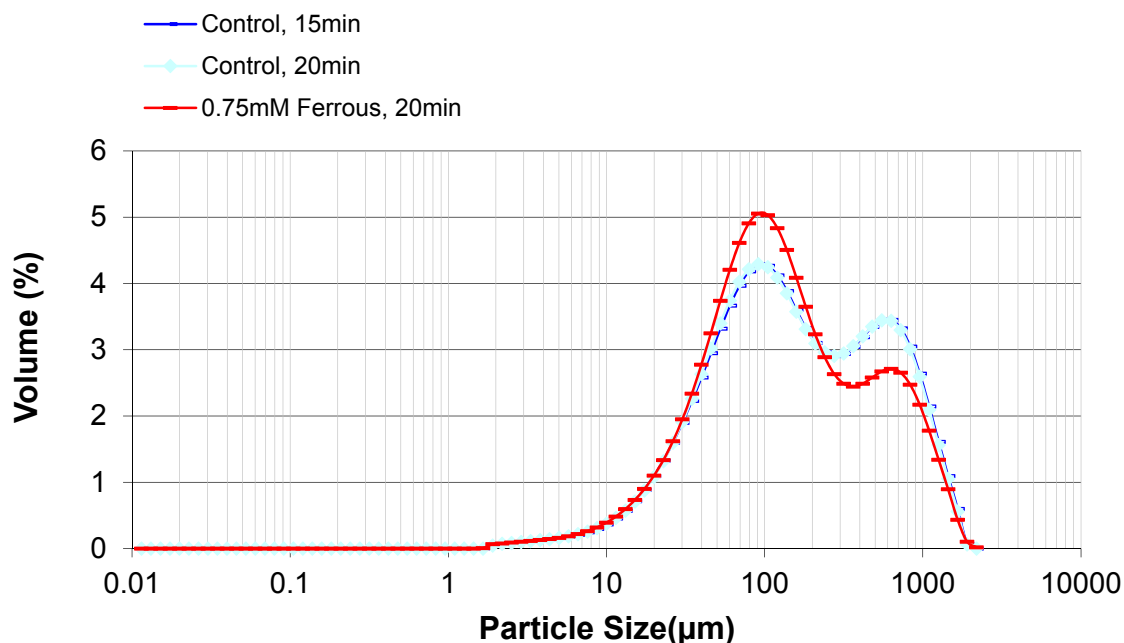


Figure 2. Particle size distribution with and without the ferrous sulfate addition.

2.2. Modelling Xylan Hydrolysis Kinetics

2.2.1. Model Prediction and Data for Xylan Hydrolysis Using 0.5% H_2SO_4

Figure 3 panel 1 shows the experimental data for control (acid-only) experiments at 150 °C, 160 °C and 170 °C for up to 30 min as well as the best-fit model predictions from Equations (3)–(6). The highest total xylan solubilization (lowest % xylan remaining in solids) occurred at 170 °C/30 min, with a total of 8% xylan remaining in the pretreated solids. At the same reaction time and temperature, the monomeric xylose yield reached a maximum (70%). However, due to the elevated temperature and residence time, roughly 13% of xylan was lost to degradation products, reducing the overall sugar yield. The highest total xylose yield (monomers plus oligomers) was thus obtained at 170 °C with a shorter residence time of 5 min, where 60% of xylan was converted to monomeric xylose and 30% to xylooligomers.

Figure 3 panel 1 also displays the biphasic behavior of xylan hydrolysis exhibited at each temperature studied. At 150 °C, 70% of xylan was hydrolyzed in the first 8 min, but only 78% was hydrolyzed after 20–25 min. At 160 °C, 80% of xylan was hydrolyzed in 10 min, with 90% converted after 30 min. At 170 °C, 85% of xylan was hydrolyzed in 5 min; however, it took another 25 min to reach 90% conversion. It is of note that the dissolved xylooligomers also show biphasic profiles. About 10% (160 °C, 170 °C) to 20% (150 °C) of xylooligomers were converted to monomers at rather slow rates.

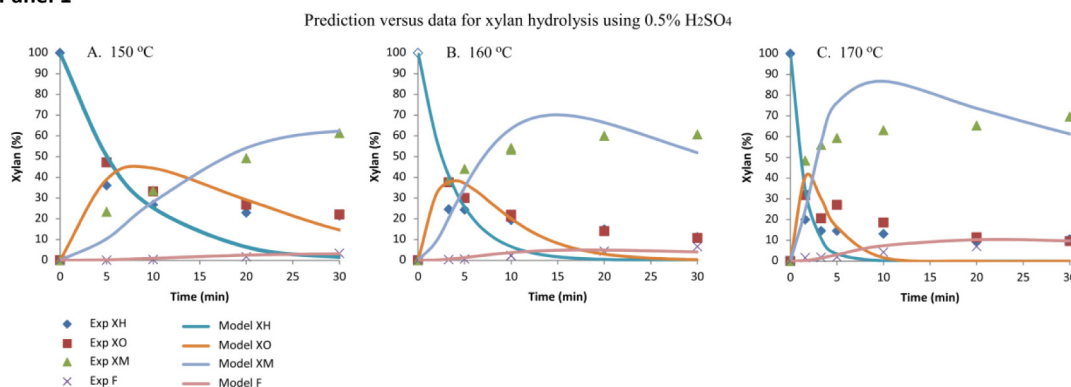
Because of the biphasic profiles of both xylan and xylooligomers, the model presented in Equation (2) accurately predicts the xylooligomer and xylose monomer yields only for the fast phase kinetic range characteristic for low temperatures and short residence times. The measured xylose monomer data was thus always lower than predicted for slower reaction phases, while the experimental xylan and xylooligomer concentrations exceeded the best-fit model predictions.

One possible explanation of the observed biphasic kinetic curves is that the acid concentration in the reactor decreases over time as steam condenses during pretreatment. This potential explanation corroborates the observed pH increase of acid-soaked biomass from 0.9–1.1 before the pretreatment to 1.9–2.1 after a 20 min steam pretreatment.

Another potential cause could be a difference in the accessibility of two xylan fractions [33]. This explanation of the observed biphasic behavior would be consistent with the general biomass

composition, as the slowly hydrolyzed fraction of xylan could be embedded within lignin or linked to lignin via lignin–carbohydrate bonds [34]. This hypothesis is supported by ultrastructure studies of biomass [35,36]. Dammström further suggested the presence of a third kind of xylan, which is tightly bound to cellulose by hydrogen bonds [35].

Panel 1



Panel 2

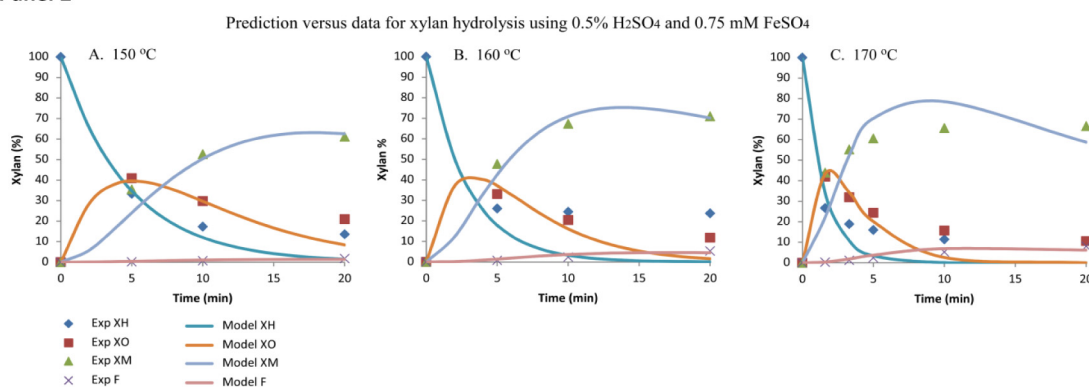


Figure 3. Best-fit model prediction and data for xylan hydrolysis using 0.5% H₂SO₄ (panel 1), and 0.5% H₂SO₄ and 0.75 mM FeSO₄ (panel 2). The modelling and experiments were for the temperature setting at (A) 150 °C, (B) 160 °C, and (C) 170 °C. XH = xylan in biomass, XO = xylooligomers, XM = xylose, F = furfural.

However, this second explanation is less consistent with the observed biphasic curves for xylooligomers. If this were the sole explanation, one would have to assume that the bulk of xylooligomers formed are of high molecular weight, as their low-molecular-weight analogs are soluble in water.

The model proposed by Morinelly et al. also found the same over-prediction of xylooligomer yields, and so the authors suggested quasiequilibrium between low-molecular-weight oligomers and xylose [32]. The reversible kinetic model was successfully applied earlier to the dilute acid hydrolysis of cellulose [37].

2.2.2. Model Prediction and Data for Xylan Hydrolysis Using 0.5% H₂SO₄ and 0.75 mM FeSO₄

Figure 3 panel 2 shows the best-fit model prediction and experimental data for xylan hydrolysis at 150 °C for up to 20 min using 0.5% H₂SO₄ with 0.75 mM FeSO₄ cocatalyst. The residual xylan amount present in the pretreated solids was as low as 8% at 170 °C, while it was about 14% at 150 °C. The highest xylose monomer yield was 70% at 160 °C, approximately 3% higher than that at 170 °C, which also produced 2% more furfural. At a pretreatment temperature of 160 °C, the xylose

yield improved by ~10% over the iron-free control. However, at 170 °C, little change was observed, suggesting that the addition of 0.75 mM FeSO₄ offers greater benefits at low-severity pretreatments. Though the cocatalyst incorporation increased the total xylan hydrolysis yield and xylose monomer yield at low severity, it did not modify the biphasic behavior discussed previously.

The kinetic model proposed in this study accurately predicted monomeric and oligomeric xylose yields at 150 °C and 160 °C (Figure 3 panel 2). Estimation of furfural aligned well with the experimental data at all three temperatures. However, the conversion of xylan to xylooligomers at higher severity was once again over-predicted. The model expected a complete hydrolysis of xylan, which was not experimentally observed. The cause of the observed biphasic behavior should be similar to those discussed above.

The reaction constants of the individual process steps, k_i , derived from best-fit predictions, are listed in Table 2. The rate constant for the conversion of xylan to xylooligomers, k_1 , nearly doubled at 150 °C when 0.75 mM Fe²⁺ was introduced. The cocatalyst addition also increased k_1 at 160 °C by nearly 25%. However, no effect of the cocatalyst addition was observed when the temperature was elevated to 170 °C. The rate constant for the conversion of xylooligomer to xylose, k_2 , was also doubled by cocatalyst addition at 150 °C, while only a slight increase was found at 160 °C. By contrast, a nearly 20% rate depression was observed between the control and cocatalyst pretreatments at 170 °C.

Even more pronounced changes were observed for the reaction rate constants of the two final steps. The degradation rate constants, k_3 and k_4 , increased with increasing temperature in control experiments. By contrast, little change was observed in k_3 in the experiments with iron, whereas k_4 actually decreased with increasing temperature.

Table 2. Fitted kinetics constants to experimental data. The control refers to the acid-alone condition, as a comparison to the treatments in which 0.75 mM Fe²⁺ is added to the acids.

	150 °C Control	150 °C 0.75 mM Fe ²⁺	160 °C Control	160 °C 0.75 mM Fe ²⁺	170 °C Control	170 °C 0.75 mM Fe ²⁺
k_1	0.137	0.212	0.272	0.343	0.698	0.674
k_2	0.090	0.182	0.250	0.272	0.584	0.470
k_3	0.019	0.033	0.030	0.025	0.036	0.033
k_4	0.367	1.488	0.408	0.403	0.481	0.337

These qualitative observations corroborate the quantitative results obtained by calculation of activation energies. Figure 4 shows the Arrhenius plots created using the reaction constants listed in Table 2 for both acid-only control and 0.75 mM ferrous cocatalyst experiments. Due to the constant acid loading across all experiments, the activation energy can be calculated from the slope of the best-fit straight line. Table 3 lists the corresponding activation energy and R² values, as detailed by Equation (7).

Table 3. Activation energy, Ea.

	Ea for Control (0.5% H ₂ SO ₄ Only) (kJ/mol)	Arrhenius Fit, R ² for Control (0.5% H ₂ SO ₄)	Ea for 0.75 mM FeSO ₄ with 0.5% H ₂ SO ₄ (kJ/mol)	Arrhenius Fit, R ² for 0.75 mM FeSO ₄ with 0.5% H ₂ SO ₄
k_1	128	0.9889	90	0.9883
k_2	146	0.9986	74	0.9900
k_3	51	0.9593	NA	NA
k_4	21	0.9807	NA	NA

NA, not applicable; current model is not able to provide meaningful results, suggesting more complex reaction mechanisms and kinetic models shall be investigated in the future.

The R² values approach unity with the exception of k_3 and k_4 . The activation energy for k_1 in control experiments was observed to be 128 kJ/mol in this study, which matches 130 kJ reported by

Garrote et al. [38,39]. It was reduced by 30% with the addition of 0.75 mM FeSO₄. The activation energy of k_2 was also significantly reduced, from 146 kJ/mol in control pretreatments to 74 kJ/mol in FeSO₄ cocatalyst pretreatments.

As seen in Table 3, the addition of the iron cocatalyst reduces the activation energies of all reaction steps, though this effect is more pronounced on the second, rate-limiting step of the acid pretreatment, that is, the conversion of xylooligomers to xylose. As a result, the prior step, xylan degradation, becomes rate limiting, although these first two steps have similar activation energies, so it is their combination that should be considered rate limiting. As for steps 3 and 4, conversion of xylose to furfural and further downstream degradation products, the lack of the Arrhenius-like behavior (Figure 4) suggests that the degradation of xylose to furfural and pseudo-lignin products in the presence of ferrous ion may not follow the postulated mechanism. This behavior could be caused by the degradation of xylose into products other than furfural (not measured in this study) as reported by Liu et al. [24].

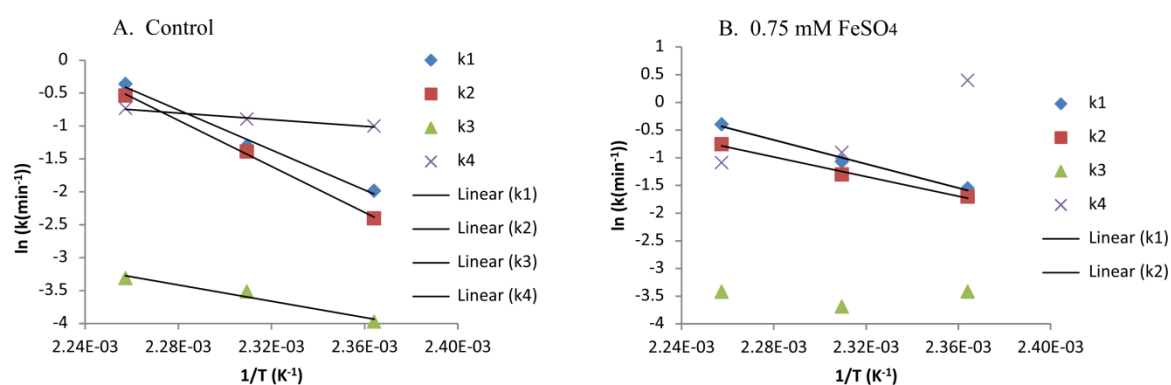


Figure 4. Arrhenius plots for control (acid alone) and 0.75 mM FeSO₄ cocatalyst pretreatment from Table 2. The analysis is presented for (A) the control, and (B) 0.75 mM FeSO₄ cocatalyst pretreatments.

2.3. Effect of Ferrous Ions on Enzymatic Hydrolysis

The impact of ferrous-iron pretreatment on high-solids enzymatic hydrolysis is depicted in Figure 5. Addition of 0.75 mM Fe²⁺ increased the glucose yield from 46.3% in control experiments to 56.3% in the experiments with cocatalyst addition. However, besides the direct effect of iron, the observed increase of the glucose yield could also be attributed to the sample alteration as a result of the prior treatment with iron, cf. Figure 2.

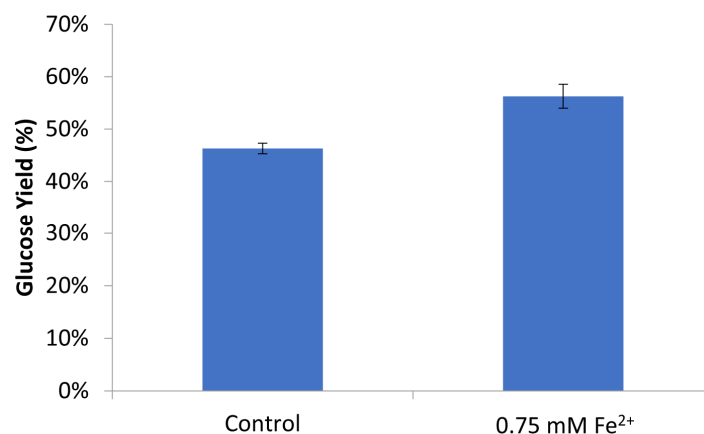


Figure 5. Glucose yield (based on glucan percent after pretreatment) during high-solids enzymatic hydrolysis on unwashed solids.

To ascertain the factor causing this effect, the effect of ferrous ions on the low-solids enzymatic hydrolysis was studied; the results are shown in Figure 6.

Unlike the whole slurry (high-solids) enzymatic hydrolysis, which is conducted without an exhaustive wash stage, thus leaving the iron ions intact, the low-solids treatment uses the same sample but includes an extensive washing stage removing the bulk of iron left over from the pretreatment. All experimental conditions showed roughly a 70% glucose yield after 96 h. A greater yield observed for low-solids hydrolysis appears to be a result of a greater sample homogeneity improving mass transfer.

In contrast to the high-solids variant, no significant effect was observed in treatments with iron, as expected due to the prior washing step. Thus the contribution of iron into the observed increase of the glucose release from the high-solids enzymatic treatment was confirmed, as the samples showed the same glucose yield with the prior iron removal.

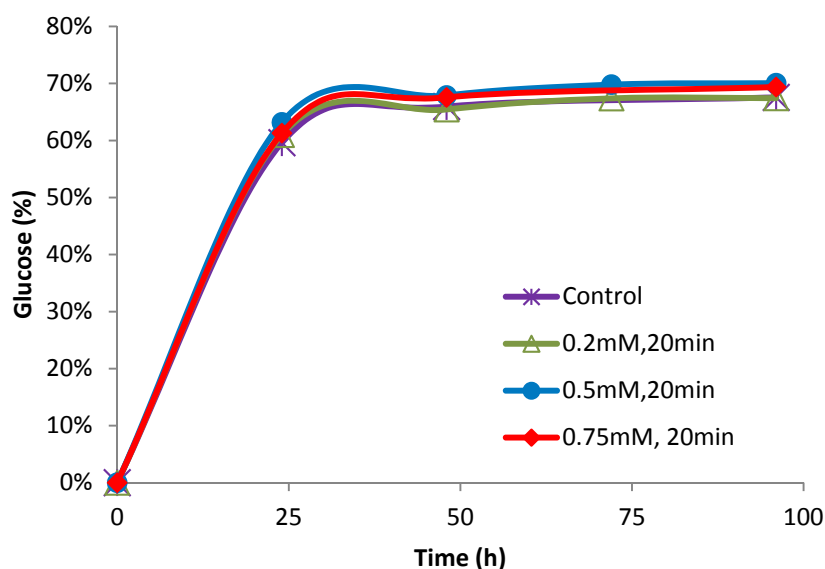


Figure 6. Glucose yield (based on glucan percent after pretreatment) during low-solids enzymatic hydrolysis on washed solids.

3. Discussion

3.1. Dilute-Acid Pretreatments under Different Temperatures and Cost Issues

In literature, a combined severity factor (CSF), which is calculated as a function of temperature, time and acid concentration, has been used to evaluate the trading off among temperature, time and acid concentration for the dilute-acid pretreatments that hydrolyze hemicellulose [40,41]. Application of the CSF concept can explain the recent reports that using relatively mild temperatures (100–130 °C) can also result in a satisfactory conversion of xylan to xylose [11,21,22], that is, the mild-temperature factor is compensated with a longer pretreatment time (1–4.5 h). In this regard, the mild- and high-temperature dilute-acid pretreatments of similar efficiency feature comparable CSFs, and the determining factor in choosing mild- versus high-temperature dilute-acid pretreatments will likely depend on the availability of heating supply and pretreatment reactors, and so on, for enabling longer reaction times.

Thus, the reported success of the mild-temperature dilute-acid pretreatments themselves will likely not ‘phase out’ the relatively high-temperature option, as the latter requires shorter pretreatment times and enables a faster pretreatment cycle that leads to a more efficient equipment utilization.

The cost of dilute-acid pretreatment can be further reduced by using Fe^{2+} as a Lewis acid (which is fairly cheap compared to sulfuric acid) or ferric chloride (which is only half the cost of hydrochloric acid). The rationale for using iron salts in pretreatment is to reduce the cost of

mineral acids. Furthermore, the newly developed iron-accumulating transgenic plants, as elaborated in detail below, can effectively eliminate the cost of supplementing the iron catalyst prior to pretreatment.

3.2. Technology Development for Iron Dilute-Acid Pretreatment: from Post-Harvest Supplementation of Iron to In-Planta Iron Accumulation

The current approach of soaking or spraying the milled biomass with iron ion solution prior to pretreatment is not ideal due to labor and equipment costs as well as diffusion limitations for infiltrating dry plant tissues with iron ions. These infiltration problems arise from the binding of iron ions to the biomass surface [42] and the presence of intracellular air-filled voids within cell wall tissues. To more effectively overcome these process limitations, our group and other groups recently used three novel approaches to deliver a metal cocatalyst into the plant cell wall region during plant growth: (1) expressed heterologous iron-storage protein ferritins intracellularly (referred to as FerIN) [43], (2) expressed ferritin extracellularly (referred to as FerEX) [44], and (3) expressed blood iron-binding peptide (BIBP) in Arabidopsis and rice plants [45]. These FerEX transgenic plants accumulated approximately 50–110% more iron under normal growth conditions, compared with the empty-vector control plants.

Remarkably, the harvested biomass of such iron transgenic plants showed enhanced pretreatability and digestibility, releasing approximately 18–21% more glucose and 13–34% more xylose than the empty-vector control plants after dilute-acid pretreatment, or hot water (which can be viewed as a weak acid) pretreatment and co-saccharification [43–45].

These approaches allow iron to accumulate in proximity to the cell wall matrix during plant growth, thereby promoting intimate association of iron and biopolymers throughout the cell wall, which will further reduce the cost of metal catalysts, increase the reactivity of the biomass, and pave the way for future development of metal catalyst-facilitated pretreatment of biomass.

3.3. Effects of Iron Dilute-Acid Pretreatment and Its Enhancement of Xylose Monomer Yield

We previously reported that, during iron-based dilute-acid pretreatment, we observed concomitant increases in solubilized sugars in the hydrolysates as well as reducing sugars in the (insoluble) biomass residues [46]. Meanwhile, the enhancements in sugar release during subsequent enzymatic saccharification of iron dilute-acid-pretreated biomass were also observed [46]. In this study, the effects of ferrous sulfate were not only reflected on the sugar releases during pretreatment, but also on the enzymatic hydrolysis of pretreated biomass residues. As shown in Figure 5, the glucose yield by the saccharification increased by nearly 10% due to the addition of iron Lewis acid. Note that this 10% increase in glucose yield was compared against the control of dilute-acid-alone pretreatment; if the non-pretreated corn stover biomass is used as an absolute control for the saccharification, the magnitude for glucose yield enhancement by the addition of iron Lewis acid would be significantly higher than 10%. Furthermore, considering the scale of a commercial plant, which processes biomass by a hundred to a thousand tons per day, a 10% increase in glucose yield using iron cocatalyst could lead to a rather large increase in revenue, thus being very attractive for biorefineries, especially so because the iron cocatalyst is used at very low cost and dosage.

One purpose of dilute-acid pretreatment of biomass is to convert as much xylan to xylose as possible. Accordingly, the dilute-acid-alone pretreatment conditions applied in this study were already suboptimized for maximal xylan conversion (e.g., 70–80% of xylan was solubilized, as shown in the controls in Figure 1). Thus, it is not surprising that further enhancement of the total xylan conversion/solubilization by the addition of iron catalyst was relatively moderate in this study. However, the xylose monomer yields by 150 °C with 0.75 mM Fe²⁺/dilute acid for all different pretreatment times (i.e., 5, 10 and 20 min) were significantly higher than the control of dilute acid alone (cf. Figure 1).

3.4. Potential Mechanisms of Iron-Based Dilute-Acid Pretreatment and Enhancement of Xylose Monomer Yield

Our previous studies showed that the iron-based dilute-acid pretreatment likely targets multiple chemical sites in plant cell wall polymer networks, including the C–O–C and C–H bonds in cellulose [46]; while the exact mechanism remains unclear, it is possible that iron ions may attack the C–O–C bonds via acid–base reactions and the C–H bonds via redox reactions. For Fe²⁺ dilute-acid-pretreated corn stover, imaging by Prussian Blue staining indicated that iron ions associated with both cellulose/xylan and lignin, whereas the analyses by scanning electron microscopy and transmission electron microscopy revealed structural details of corn stover after Fe²⁺ dilute-acid pretreatment, that is, delamination and fibrillation of cell walls [46].

Furthermore, it was reported that cellulose treated at 0.5 mM concentration of Fe²⁺ and 2% concentration of H₂O₂ for a reaction period of 48 h enhanced cellulose depolymerization through the Fenton reaction [47]. The addition of iron into dilute-acid pretreatment may also enable the air/oxygen-driven Fenton reaction to depolymerize cellulose during pretreatment, and future studies are needed to explore this possibility.

A recent review highlighted the multiple roles that iron catalysts play in organic synthesis [48]; it is reasonable to speculate that the iron cocatalysts likely also conduct multiple, complex tasks in the process of biomass pretreatment. This is in line with our previous studies showing that the iron catalyst may target multiple chemistries in plant cell wall polymer networks as described above. In addition, iron cocatalysts may also impact lignin redeposition. With our current kinetic data, we may not be able to correlate much to the involved mechanisms, but the planned future work aided by ultrastructural and molecular studies would help us reveal more mechanistic details of iron cocatalysis.

4. Materials and Methods

4.1. Raw Material and Its Compositional Analysis

Whole corn stover (Pioneer variety 33A14) was harvested in 2002 and tub ground at the Kramer farm in Wray, Colorado, USA, then further milled at NREL (National Renewable Energy Laboratory) through a Mitts & Merrill rotary knife mill (model 10 × 12) to pass a $\frac{1}{4}$ -inch screen. The solids compositional analysis of $\frac{1}{4}$ -inch milled corn stover was conducted using the NREL LAP (Laboratory Analytical Procedure) [49], and is reported in Table 4. Note that Table 4 has more components (i.e., columns) than applicable to treated biomass, for example, structural proteins, sucrose, water extractable, ethanol extractives, and so on.

Table 4. Solids compositional analysis of native corn stover.

Feedstock	Structural Protein (%)	Sucrose (%)	Water-Extractable Others (%)	Ethanol Extractives (%)	Lignin (%)	Glucan (%)	Xylan (%)	Galactan (%)	Arabinan (%)	Mannan (%)	Uronic Acid (%)	Acetyl (%)	Total (%)
Corn stover 33A14	1.6	4.0	6.1	2.2	12.3	34.0	22.0	1.6	3.1	0.0	3.7	2.9	99.1

4.2. Process Water

Process water used for impregnation was analyzed using inductively coupled plasma-optical emission spectroscopy (ICP-OES) by the Chemical Analysis Laboratory at the University of Georgia, and found to contain less than 2 μM iron.

4.3. Impregnation

Acid impregnation was carried out using a recirculating atmospheric pressure impregnation (RAPI) system as described by Tucker et al. [50]. Approximately 120 L of warm (48 °C to 50 °C), 0.5 wt % H_2SO_4 was placed in the recirculation tank and sparged with argon for 20 min before a measured amount of iron sulfate (FeSO_4) was added. A Hastelloy C-276 wire mesh (20 mesh screen) basket was loaded with 6 to 14.5 kg of $\frac{1}{4}$ -inch milled corn stover feedstock (~94% solids) and immersed in a warm dilute acid/cocatalyst bath for 2 h. The argon sparge was used to purge oxygen gas from the acid solution prior to the addition of the Fe^{2+} reagent. Past experience has shown that the Fe^{2+} ions oxidize quickly in aqueous solutions, resulting in the formation of an insoluble precipitate if the solution was not sparged with argon or nitrogen prior to the Fe^{2+} salt addition.

Following each respective acid impregnation, the feedstock was suspended in the basket and drained of excess liquid (to approximately 20% solids), loaded into the mold of a hydraulic dewatering press (also sparged with argon), and pressed to ~43% solids. The acid/cocatalyst-impregnated feedstock was prepared on the same day as the pretreatment experiments were conducted in order to minimize the potential oxidation of Fe^{2+} .

4.4. Bench-Scale Pretreatment

A 4-liter steam explosion reactor (NREL Digester, Autoclave Engineers Group, Erie, PA, USA) was used for all pretreatment experiments. The NREL Digester was pre-heated to an allotted pretreatment temperature and sparged with argon for 1 min using a lance that reached the bottom of the reactor. Following sparging, the digester was loaded with 500.0 g of dewatered feedstock (~40% to 45% solids) and quickly reheated (~5 to 10 s) via direct steam injection. Pretreatment experiments were carried out at 150 °C, 160 °C and 170 °C, 0.5 wt % H_2SO_4 , and 5, 10, 20, 30 and 40 min residence times. The ferrous sulfate cocatalyst was added at concentrations of 0.2 mM, 0.5 mM, 0.75 mM and 1.0 mM, with virtually no change in the pH of the acid solution. The above range of ferrous sulfate concentrations was chosen for the following reasons: firstly, our previous studies have shown that ferrous sulfate in the concentration range of 0.2–25.0 mM was effective in enhancing the dilute-acid pretreatment of biomass [23,46], in which ferrous sulfate at as low as 0.2 mM concentration already provided good improvement on sugar yields [23]. Secondly, the use of higher ferrous sulfate concentrations may lead to higher degradation products such as HMF (Hydroxymethylfurfural) and furfural. Thus, a concentration range of 0.2–1.0 mM ferrous sulfate was used in this study.

Xylan mass balance closure was carried out for the pretreatments conducted at 150 °C with an impregnation acid concentration of 0.5% H_2SO_4 and cocatalyst concentrations of 0, 0.2 mM, 0.5 mM, 0.75 mM and 1 mM ferrous sulfate for 5 min, 10 min and 20 min. The amounts of xylan, its oligomers and monomer (xylose), and furfural were assessed. For the measurement of xylooligomer, we followed the NREL LAP [49] in measuring the total dissolved xylose before and after 4% acid hydrolysis in the liquid phase; the difference was deemed the amount of xylooligomer that dissolved.

4.5. High-Solids Enzymatic Hydrolysis of Unwashed Solids

Enzymatic hydrolysis was conducted at 15% solids using unwashed whole slurries produced in pretreatment. Pretreated slurry (125 g) was first diluted with 75% of the calculated water required to achieve a 15% solids loading. The slurry then was adjusted to a pH of 5.0 by slowly adding 28% ammonium hydroxide (NH_4OH) to the continually stirred slurry. If the pH rose above 5.0 during neutralization, 10 M sulfuric acid (H_2SO_4) was added to correct the pH to 5.0. The neutralized

slurry was then diluted to 15% solids with deionized water. Then, 60 g of this slurry was loaded into 125 mL polypropylene roller bottles with 20 mg protein (Genencor GC220, Lot # 4900759448, Genencor International Inc., Rochester, NY, USA) per g cellulose. Samples were incubated for 112 h at 50 °C, and the bottles were rolled at 4 rpm.

4.6. Low-Solids Enzymatic Hydrolysis of Washed Solids

Low-solids enzymatic digestion of washed pretreated solids from the pretreatment experiments was performed in 125 mL Erlenmeyer shake flasks at 1% cellulose solids loading (approximately 2 wt % solids loadings), 50 °C, and 130 rpm, as specified in NREL Laboratory Analytical Procedures (LAP) [51]. The washed residues were obtained following the extensive washing procedure for FIS (fraction of insoluble solids), as previously described [49]. Genencor GC220 cellulase enzyme cocktail was added at a loading of 20 mg of protein per gram of cellulose. No additional β -glucosidase or xylanase (Multifect Xylanase, Lot # 301-02300-197, Genencor International Inc., Rochester, NY, USA) was added. The total volume of the saccharification slurries after adding the enzyme and buffer was 50 mL. Saccharification samples were taken at 24, 48, 72, 96 and 168 h and analyzed by HPLC (High Performance Liquid Chromatography) for glucose and xylose content.

4.7. Analyses of Liquors and Solid Residues

Pretreatment liquors were analyzed using HPLC according to NREL LAPs [52,53]. Solid residues were analyzed according to NREL LAP [49]. Fraction-insoluble solids (FIS) were obtained following the exhaustive washing procedure described in the NREL LAP [49].

4.8. Data Modelling

The kinetic equations derived from Equation (2) are listed in Table 5. The differential equation system was solved symbolically as reported by Morinelly et al. [32]. The equations were fitted to the corresponding data simultaneously using a quasi-Newtonian method in Excel solver. The four kinetic constants, k_1 through k_4 , were calculated to optimize the model fit.

Table 5. Kinetic equations developed from Equation (2).

Equations	No.	Boundary Conditions (Sugar Yield)
$\frac{dXH(t)}{dt} = -k_1XH(t)$	Equation (3)	$XH(0) = 100\%$
$\frac{dXO(t)}{dt} = k_1XH(t) - k_2XO(t)$	Equation (4)	$XO(0) = 0\%$
$\frac{dXM(t)}{dt} = k_2XO(t) - k_3X(t)$	Equation (5)	$X(0) = 0\%$
$\frac{dX(t)}{dt} = k_3X(t) - k_4F(t)$	Equation (6)	$F(0) = 0\%$

The kinetic constants should obey the Arrhenius equation, which is a function of temperature (T , absolute temperature) and acid concentration, as shown in Equation (7) [32]. To simplify the model, the acid concentration was held constant (0.5 wt %) in the current study. The activation energy for each of the four reactions was then calculated from the appropriate plot.

$$k_i = A_i c^m \exp\left(-\frac{E_i}{RT}\right), \quad (7a)$$

which simplifies to the classical Arrhenius equation at a constant acid concentration:

$$k_i = B_i \exp\left(-\frac{E_i}{RT}\right), \quad (7b)$$

where

- T = temperature (K);

- B = pre-exponential factor (min^{-1});
- c = acid concentration (wt %);
- m = acid concentration exponent (unitless);
- E = activation energy (kJ/mol);
- R = 8.314 J/mol·K.

5. Conclusions

Iron(II) sulfate speeds up both the xylan hydrolysis during acidic biomass pretreatment and glucose release during the subsequent enzymatic hydrolysis of cellulose, as long as iron is not washed out of the pretreated biomass. The conducted kinetic modelling and calculation of activation energies showed that iron cocatalyst appears to accelerate all pertinent reactions of xylan decomposition including those of xylose and furfural decomposition. Thus, conducting the process at lower temperatures yet long residence times is recommended to maximize the yield of sugars.

Acknowledgments: We would like to acknowledge the funding support from the BioEnergy Technologies Office (BETO) program in the U.S. DOE Office of Energy Efficiency and Renewable Energy (EERE) under the contract # DE-AC36-08GO28308. The metal catalyst enhancement on biomass pretreatment were also supported by the Center for Direct Catalytic Conversion of Biomass to Biofuels (C3Bio), an Energy Frontier Research Center funded by the DOE Office of Science, Office of Basic Energy Sciences (Award Number DE-SC0000997). The Alliance for Sustainable Energy, LLC (Alliance), is the manager and operator of the National Renewable Energy Laboratory (NREL). Employees of the Alliance, under Contract No. DE-AC36-08GO28308 with the U.S. Dept. of Energy, have authored this work. The United States Government retains and the publisher, by accepting the article for publication, acknowledges that the United States Government retains a non-exclusive, paid-up, irrevocable, worldwide license to publish or reproduce the published form of this work, or allow others to do so, for United States Government purposes.

Author Contributions: M.P.T., X.C. and M.E.H. led the project and coordinated the study. X.C. and M.P.T. conceived and designed the experiments. X.C., H.W., J.S., E.K. and Y.J. executed the biomass pretreatment and saccharification experiments. X.C. conducted the modelling analysis; W.W. conducted the particle size analysis. E.K. participated in the data analysis. X.C. and H.W. prepared, and M.P.T., Y.J. and E.K. edited the manuscripts; H.W. coordinated the manuscript submission. All authors read and approved the final manuscript.

Conflicts of Interest: The authors declare no conflict of interest.

References

1. Fengel, D.; Wegener, G. *Wood—Chemistry, Ultrastructure, Reactions*; Walter de Gruyter: New York, NY, USA, 1984.
2. Aden, A.; Ruth, M.; Ibsen, K.; Jechura, J.; Neeves, K.; Sheehan, J.; Wallace, B.; Montague, L.; Slayton, A.; Lukas, J. *Lignocellulosic Biomass to Ethanol Process Design and Economics Utilizing Co-Current Dilute Acid Prehydrolysis and Enzymatic Hydrolysis for Corn Stover*; NREL/TP-510-32438; National Renewable Energy Laboratory: Golden, CO, USA, 2002.
3. Humbird, D.; Davis, R.; Tao, L.; Kinchin, C.; Hsu, D.; Aden, A.; Schoen, P.; Lukas, J.; Olthof, B.; Worley, M.; et al. *Process Design and Economics for Biochemical Conversion of Lignocellulosic Biomass to Ethanol: Dilute-Acid Pretreatment and Enzymatic Hydrolysis of Corn Stover*; NREL/TP-510-47764; National Renewable Energy Laboratory: Golden, CO, USA, 2011.
4. Wyman, C.E. What is (and is not) vital to advancing cellulosic ethanol. *Trends Biotechnol.* **2007**, *25*, 153–157. [[CrossRef](#)] [[PubMed](#)]
5. Rogers, P.; Lee, K.; Tribe, D. Kinetics of alcohol production by *Zymomonas mobilis* at high sugar concentrations. *Biotechnol. Lett.* **1979**, *1*, 165–170. [[CrossRef](#)]
6. Schell, D.J.; Farmer, J.; Newman, M.; McMillan, J.D. Dilute-sulfuric acid pretreatment of corn stover in pilot-scale reactor: Investigation of yields, kinetics, and enzymatic digestibilities of solids. *Appl. Biochem. Biotechnol.* **2003**, *105*, 69–86. [[CrossRef](#)]
7. Himmel, M.E.; Ding, S.-Y.; Johnson, D.K.; Adney, W.S.; Nimlos, M.R.; Brady, J.W.; Foust, T.D. Biomass recalcitrance: Engineering plants and enzymes for biofuels production. *Science* **2007**, *315*, 804–807. [[CrossRef](#)] [[PubMed](#)]

8. Serrano-Ruiz, J.C.; West, R.M.; Dumesic, J.A. Catalytic conversion of renewable biomass resources to fuels and chemicals. *Annu. Rev. Chem. Biomol. Eng.* **2010**, *1*, 79–100. [[CrossRef](#)] [[PubMed](#)]
9. Kumar, A.K.; Sharma, S. Recent updates on different methods of pretreatment of lignocellulosic feedstocks: A review. *Bioresour. Bioprocess* **2017**, *4*. [[CrossRef](#)] [[PubMed](#)]
10. Yan, X.; Wang, Z.; Zhang, K.; Si, M.; Liu, M.; Chai, L.; Liu, X.; Shi, Y. Bacteria-enhanced dilute-acid pretreatment of lignocellulosic biomass. *Bioresour. Technol.* **2017**, *245*, 419–425. [[CrossRef](#)] [[PubMed](#)]
11. Nair, R.B.; Kalif, M.; Ferreira, J.A.; Taherzadeh, M.J.; Lennartsson, P.R. Mild-temperature dilute-acid pretreatment for integration of first and second generation ethanol processes. *Bioresour. Technol.* **2017**, *245*(Part A), 145–151. [[CrossRef](#)] [[PubMed](#)]
12. Sievers, D.A.; Kuhn, E.M.; Tucker, M.P.; McMillan, J.D. Effects of dilute-acid pretreatment conditions on filtration performance of corn stover hydrolyzate. *Bioresour. Technol.* **2017**, *243*, 474–480. [[CrossRef](#)] [[PubMed](#)]
13. Teramura, H.; Sasaki, K.; Kawaguchi, H.; Matsuda, F.; Kikuchi, J.; Shirai, T.; Sazuka, T.; Yamasaki, M.; Takumi, S.; Ogino, C. Differences in glucose yield of residues from among varieties of rice, wheat, and sorghum after dilute-acid pretreatment. *Biosci. Biotechnol. Biochem.* **2017**, *81*, 1–7. [[CrossRef](#)] [[PubMed](#)]
14. Deshavath, N.N.; Mohan, M.; Veeranki, V.D.; Goud, V.V.; Pinnamaneni, S.R.; Benarjee, T. Dilute-acid pretreatment of sorghum biomass to maximize the hemicellulose hydrolysis with minimized levels of fermentative inhibitors for bioethanol production. *3 Biotech.* **2017**, *7*, 139. [[CrossRef](#)] [[PubMed](#)]
15. Lehto, J.; Louhelainen, J.; Huttunen, M.; Alen, R. Spectroscopic analysis of hot-water- and dilute-acid-extracted hardwood and softwood chips. *Spectrochim. Acta Part A Mol. Biomol. Spectrosc.* **2017**, *184*, 184–190. [[CrossRef](#)] [[PubMed](#)]
16. Hu, B.-B.; Zhu, M.-J. Direct hydrogen production from dilute-acid pretreated sugarcane bagasse hydrolysate using the newly isolated *Thermoanaerobacterium thermosaccharolyticum* MJ1. *Microb. Cell Fact.* **2017**, *16*, 77. [[CrossRef](#)] [[PubMed](#)]
17. Azizi, N.; Najafpour, G.; Younesi, H. Acid pretreatment and enzymatic saccharification of brown seaweed for polyhydroxybutyrate (phb) production using cupriavidus necator. *Int. J. Biol. Macromol.* **2017**, *101*, 1029–1040. [[CrossRef](#)] [[PubMed](#)]
18. Kapoor, M.; Soam, S.; Agrawal, R.; Gupta, R.P.; Tuli, D.K.; Kumar, R. Pilot scale dilute-acid pretreatment of rice straw and fermentable sugar recovery at high solid loadings. *Bioresour. Technol.* **2017**, *224*, 688–693. [[CrossRef](#)] [[PubMed](#)]
19. Chen, X.; Kuhn, E.; Jennings, E.W.; Nelson, R.; Tao, L.; Zhang, M.; Tucker, M.P. Dmr (deacetylation and mechanical refining) processing of corn stover achieves high monomeric sugar concentrations (230 g l⁻¹) during enzymatic hydrolysis and high ethanol concentrations (>10% v/v) during fermentation without hydrolysate purification or concentration. *Energy Environ. Sci.* **2016**, *9*, 1237–1245.
20. Chen, X.; Shekiri, J.; Pschorn, T.; Sabourin, M.; Tao, L.; Elander, R.; Park, S.; Jennings, E.; Nelson, R.; Trass, O.; et al. A highly efficient dilute alkali deacetylation and mechanical (disc) refining process for the conversion of renewable biomass to lower cost sugars. *Biotechnol. Biofuels* **2014**, *7*, 98. [[CrossRef](#)]
21. Amirkhani, H.; Yunus, R.; Rashid, U.; Salleh, S.F.; Radhiah, A.D.; Syam, S. Low-temperature dilute acid hydrolysis of oil palm frond. *Chem. Eng. Commun.* **2015**, *202*, 1235–1244. [[CrossRef](#)]
22. Hong, E.; Kim, J.; Rhie, S.; Ha, S.-J.; Kim, J.; Ryu, Y. Optimization of dilute sulfuric acid pretreatment of corn stover for enhanced xylose recovery and xylitol production. *Biotechnol. Bioprocess Eng.* **2016**, *21*, 612–619. [[CrossRef](#)]
23. Nguyen, Q.A.; Tucker, M. Dilute Acid/Metal Salt Hydrolysis of Lignocellulosics. U.S. Patent 6,423,145, 23 July 2002.
24. Liu, L.; Sun, J.; Cai, C.; Wang, S.; Pei, H.; Zhang, J. Corn stover pretreatment by inorganic salts and its effects on hemicellulose and cellulose degradation. *Bioresour. Technol.* **2009**, *100*, 5865–5871. [[CrossRef](#)] [[PubMed](#)]
25. Liu, C.; Wyman, C.E. The enhancement of xylose monomer and xylotriose degradation by inorganic salts in aqueous solutions at 180 °C. *Carbohydr. Res.* **2006**, *341*, 2550–2556. [[CrossRef](#)] [[PubMed](#)]
26. Chen, L.; Chen, R.; Fu, S. FeCl₃ pretreatment of three lignocellulosic biomass for ethanol production. *ACS Sustain. Chem. Eng.* **2015**, *3*, 1794–1800. [[CrossRef](#)]
27. Zhang, H.; Ye, G.; Wei, Y.; Li, X.; Zhang, A.; Xie, J. Enhanced enzymatic hydrolysis of sugarcane bagasse with ferric chloride pretreatment and surfactant. *Bioresour. Technol.* **2017**, *229*, 96–103. [[CrossRef](#)] [[PubMed](#)]
28. Kim, Y.; Yu, A.; Han, M.; Choi, G.W.; Chung, B. Ethanosolv pretreatment of barley straw with iron(III) chloride for enzymatic saccharification. *Chem. Technol. Biotechnol.* **2010**, *85*, 1494–1498. [[CrossRef](#)]

29. Liu, H.; Zhu, J.Y.; Fu, S.Y. Effects of lignin–metal complexation on enzymatic hydrolysis of cellulose. *J. Agric. Food Chem.* **2010**, *58*, 7233–7238. [[CrossRef](#)] [[PubMed](#)]
30. Degenstein, J.; Reddy Kamireddy, S.; Tucker, M.P.; Ji, Y. Oligomer saccharide reduction during dilute-acid pretreatment co-catalyzed with lewis acids on corn stover biomass. *Int. J. Agric. Biol. Eng.* **2013**, *6*, 54–62.
31. Saeman, J.F. Kinetics of wood saccharification—Hydrolysis of cellulose and decomposition of sugars in dilute acid at high temperature. *Ind. Eng. Chem.* **1945**, *37*, 43–52. [[CrossRef](#)]
32. Morinelly, J.E.; Jensen, J.R.; Browne, M.; Co, T.B.; Shonnard, D.R. Kinetic characterization of xylose monomer and oligomer concentrations during dilute-acid pretreatment of lignocellulosic biomass from forests and switchgrass. *Ind. Eng. Chem. Res.* **2009**, *48*, 9877–9884. [[CrossRef](#)]
33. Conner, A.H. Kinetic modeling of hardwood prehydrolysis. Part I. Xylan removal by water prehydrolysis. *Wood Fiber Sci.* **1984**, *16*, 268–277.
34. Adler, E. Lignin chemistry—Past, present and future. *Wood Sci. Technol.* **1977**, *11*, 169–218. [[CrossRef](#)]
35. Dammstrom, S.; Salmen, L.; Gatenholm, P. On the interactions between cellulose and xylan, a biomimetic simulation of the hardwood cell wall. *Bioresources* **2009**, *4*, 3–14.
36. Reis, D.I.; Vian, B. Helicoidal pattern in secondary cell walls and possible role of xylans in their construction. *Comptes Rendus Biol.* **2004**, *327*, 785–790. [[CrossRef](#)]
37. Abatzoglov, N.; Bouchard, J.; Chornet, E.; Overend, R.P. Dilute acid depolymerization of cellulose in aqueous phase: Experimental evidence of the significant presence of soluble oligomeric intermediates. *Can. J. Chem. Eng.* **1986**, *64*, 781–786. [[CrossRef](#)]
38. Garrote, G.; Domínguez, H.; Parajó, J.C. Interpretation of deacetylation and hemicellulose hydrolysis during hydrothermal treatments on the basis of the severity factor. *Process Biochem.* **2002**, *37*, 1067–1073. [[CrossRef](#)]
39. Garrote, G.; Domínguez, H.; Parajo, J. Autohydrolysis of corncob: Study of non-isothermal operation for xylooligosaccharide production. *J. Food Eng.* **2002**, *52*, 211–218. [[CrossRef](#)]
40. Schell, D.J.; Farmer, J.; Newman, M.; McMillan, J.D. Dilute-sulfuric acid pretreatment of corn stover in pilot-scale reactor. In *Biotechnology for Fuels and Chemicals*; Springer: New York, NY, USA, 2003; pp. 69–85.
41. Wyman, C.E.; Yang, B. Combined severity factor for predicting sugar recovery in acid-catalyzed pretreatment followed by enzymatic hydrolysis. In *Hydrothermal Processing in Biorefineries*; Springer: New York, NY, USA, 2017; pp. 161–180.
42. Zelinka, S.L.; Gleber, S.-C.; Vogt, S.; Rodriguez Lopez, G.M.; Jakes, J.E. Threshold for ion movements in wood cell walls below fiber saturation observed by X-ray fluorescence microscopy (XFM). *Holzforschung* **2015**, *69*, 441–448. [[CrossRef](#)]
43. Wei, H.; Yang, H.; Ciesielski, P.N.; Donohoe, B.S.; McCann, M.C.; Murphy, A.S.; Peer, W.A.; Ding, S.-Y.; Himmel, M.E.; Tucker, M.P. Transgenic ferritin overproduction enhances thermochemical pretreatments in arabidopsis. *Biomass Bioenerg.* **2015**, *72*, 55–64. [[CrossRef](#)]
44. Lin, C.-Y.; Jakes, J.E.; Donohoe, B.S.; Ciesielski, P.N.; Yang, H.; Gleber, S.-C.; Vogt, S.; Ding, S.-Y.; Peer, W.A.; Murphy, A.S.; et al. Directed plant cell-wall accumulation of iron: embedding cocatalyst for efficient biomass conversion. *Biotechnol. Biofuels* **2016**, *9*. [[CrossRef](#)] [[PubMed](#)]
45. Yang, H.; Wei, H.; Ma, G.; Antunes, M.S.; Vogt, S.; Cox, J.; Zhang, X.; Liu, X.; Bu, L.; Charlotte, G.S.; et al. Cell wall targeted in planta iron accumulation enhances biomass conversion and seed iron concentration in arabidopsis and rice. *Plant Biotechnol. J.* **2016**, *14*. [[CrossRef](#)] [[PubMed](#)]
46. Wei, H.; Donohoe, B.S.; Vinzant, T.B.; Ciesielski, P.N.; Wang, W.; Gedvilas, L.M.; Zeng, Y.; Johnson, D.K.; Ding, S.Y.; Himmel, M.E.; et al. Elucidating the role of ferrous ion cocatalyst in enhancing dilute-acid pretreatment of lignocellulosic biomass. *Biotechnol. Biofuels* **2011**, *4*, 48. [[CrossRef](#)] [[PubMed](#)]
47. Jain, P.; Vigneshwaran, N. Effect of Fenton’s pretreatment on cotton cellulosic substrates to enhance its enzymatic hydrolysis response. *Bioresour. Technol.* **2012**, *103*, 219–226. [[CrossRef](#)] [[PubMed](#)]
48. Bauer, I.; Knölker, H.-J. Iron catalysis in organic synthesis. *Chem. Rev.* **2015**, *115*, 3170–3387. [[CrossRef](#)] [[PubMed](#)]
49. Sluiter, A.; Hyman, D.; Payne, C.; Wolfe, J. *Determination of Insoluble Solids in Pretreated Biomass Material Laboratory Analytical Procedure (LAP)*; Technical report NREL/TP-510-42627; National Renewable Energy Laboratory: Golden, CO, USA, 2008. Available online: <https://www.nrel.gov/docs/gen/fy08/42627.pdf> (accessed on 18 January 2018).

50. Tucker, M.P.; Kim, K.H.; Newman, M.M.; Nguyen, Q.A. Effects of temperature and moisture on dilute-acid steam explosion pretreatment of corn stover and cellulase enzyme digestibility. *Appl. Biochem. Biotechnol.* **2003**, *105*, 165–178. [[CrossRef](#)]
51. Selig, M.; Weiss, N.; Ji, Y. *Enzymatic Saccharification of Lignocellulosic Biomass. Laboratory Analytical Procedure (LAP)*; NERL/TP-510-42629; National Renewable Energy Laboratory: Golden, CO, USA, 2008.
52. Sluiter, A.; Hames, B.; Ruiz, R.; Scarlata, C.; Sluiter, J.; Templeton, D. *Determination of Sugars, Byproducts, and Degradation Products in Liquid Fraction Process Samples*; National Renewable Energy Laboratory: Golden, CO, USA, 2006.
53. Hyman, D.; Sluiter, A.; Crocker, D.; Johnson, D.; Sluiter, J.; Black, S.; Scarlata, C. *Determination of Acid Soluble Lignin Concentration Curve by UV-Vis Spectroscopy Laboratory Analytical Procedure (LAP)*; National Renewable Energy Laboratory: Golden, CO, USA, 2008; 13p.



© 2018 by the authors. Licensee MDPI, Basel, Switzerland. This article is an open access article distributed under the terms and conditions of the Creative Commons Attribution (CC BY) license (<http://creativecommons.org/licenses/by/4.0/>).